Synthesis design of artificial magnetic metamaterials using a genetic algorithm

P. Y. Chen[1*], C. H. Chen[2], H. Wang[2], J. H. Tsai[1], and W. X. Ni[3]

[1] *National Nano Device Laboratories, Hsinchu 30078, Taiwan R. O. C.*
[2] *Department of Computer Science, National Chiao-Tung University, Hsinchu 30050, Taiwan R.O. C.*
[3] *Department of Physics, Linköping University, S-581 83 Linköping, Sweden*
[*] *Corresponding author: pychen@mail.ndl.org.tw*

Abstract: In this article, we present a genetic algorithm (GA) as one branch of artificial intelligence (AI) for the optimization-design of the artificial magnetic metamaterial whose structure is automatically generated by computer through the filling element methodology. A representative design example, metamaterials with permeability of negative unity, is investigated and the optimized structures found by the GA are presented. It is also demonstrated that our approach is effective for the synthesis of functional magnetic and electric metamaterials with optimal structures. This GA-based optimization-design technique shows great versatility and applicability in the design of functional metamaterials.

OCIS codes: (160.3918) Metamaterials; (350.4010) Microwaves

References and links

1. J. B. Pendry, A. J. Holden, W. J. Stewart, and I. Youngs, "Extremely low frequency plasmons in metallic mesostructures," Phys. Rev. Lett. **76**, 4773-4776 (1996).
2. J. B. Pendry, A. J. Holden, D. J. Robbins, and W. J. Stewart, "Magnetism from conductors and enhanced nonlinear phenomena," IEEE Trans. Microwave Theory Tech. **47**, 2075-2084 (1999).
3. D. R. Smith, W. J. Padilla, D. C. Vier, S. C. Nemat-Nasser, and S. Schultz, "Composite medium with simultaneously negative permeability and permittivity," Phys. Rev. Lett. **84**, 4184-4187 (2000).
4. D. R. Smith and N. Kroll, "Negative refractive index in left-handed materials," Phys. Rev. Lett. **85**, 2933-2936 (2000).
5. J. B. Pendry, "Negative refraction makes a perfect lens," Phys. Rev. Lett. **85**, 3966-3969 (2000).
6. R. A. Shelby, D. R. Smith, and S. Schultz, "Experimental verification of a Negative Index of Refraction," Science **292**, 77-79 (2001).
7. T. Koschny, P. Markos, D. R. Smith, and C. M. Soukoulis, "Resonant and antiresonant frequency dependence of the effective parameters of metamaterials," Phys. Rev. E **68**, 065602-1-4 (2003).
8. T. Koschny, M. Kafesaki, E. N. Economou, and C. M. Soukoulis, "Effective medium theory of left-handed materials," Phys. Rev. Lett. **93**, 107402-1-4 (2004).
9. D. Schurig, J. J. Mock, B. J. Justice, S. A. Cummer, J. B. Pendry, A. F. Starr, and D. R. Smith, "Metamaterial electromagnetic cloak at microwave frequencies," Science **314**, 977-980 (2006).
10. W. Zhu, X. Zhao, and N. Ji, "Double bands of negative refractive index in the left-handed metamaterials with asymmetric defects," Appl. Phys. Lett. **90**, 011911-1-3 (2007).
11. H. Chen, L. Ran, J Huangfu, X. Zhang, and K. Chen, "Left-handed materials composed of only S-shaped resonators," Phys. Rev. E **70**, 057605-1-4 (2004).
12. H. Chen, L. Ran, J. Huangfu, X. Zhang, K. Chen, T. M. Grzegorczyk, and J. A. Kong, "Negative refraction of a combined double S-shaped metamaterial," Appl. Phys. Lett. **86**, 151909-1-3 (2005).
13. K. Aydin, Z. Li, M. Hudlička, S. A. Tretyakov, and E. Ozbay, "Transmission characteristics of bianisotropic metamaterials based on omega shaped metallic inclusions," New J. Phys. **9**, 326-336 (2007).
14. X. Zhou, Q. H. Fu, J. Zhao, Y. Yang, and X. P. Zhao, "Negative permeability and subwavelength focusing of quasi-periodic dendritic cell metamaterials," Opt. Express **14**, 7188-7197 (2006).
15. M. Kafesaki, T. Koschny, R. S. Penciu, T. F. Gundogdu, E. N. Economou, and C. M. Soukoulis, "Left-handed metamaterials: detailed numerical studies of the transmission properties," J. Opt. A: Pure Appl. Opt. **7**, S12-S22 (2005).

#91496 - $15.00 USD Received 8 Jan 2008; revised 15 Mar 2008; accepted 17 Mar 2008; published 8 Aug 2008

16. F. J. Ville, T. Cwik, Y. Rahmat-Samii, and M. Manteghi, "A parallel electromagnetic genetic-algorithm optimization (EGO) application for patch antenna design," IEEE Trans. Antenna Propag. **52**, 2424-2435 (2004).
17. D. J. Kern, D. H. Werner, and M. Lisovich, "Metaferrites using electromagnetic bandgap structures to synthesis metamaterial ferrites," IEEE Trans. Antenna Propag. **53**, 1382-1389 (2005).
18. J. W. Rinne and P. Wiltzis, "Design of holographic structures using Genetic Algorithm," Opt. Express **14**, 9909-9916 (2006).
19. J. Goh, I. Fushman, D. Englund, and J. Vuckovic, "Genetic optimization of photonic band structures," Opt. Express **15**, 8218-8230 (2007).
20. P. Y. Chen, C. H. Chen, J. S. Wu, H. C. Wen, and W. P. Wang, "Optimal design of integrally gated CNT field-emission devices using a genetic algorithm," Nanotechnology **18**, 395203-1-10 (2007).
21. D. H. Kwon and D .H. Werner, "Low-index metamaterial designs in visible spectrum," Opt. Express **14**, 9267-9272 (2007)
22. G. Mumcu, M. Valerio, K. Sertel, and J. L. Volakis, "Applications of the finite element method to designing composite metamaterials," International conference on electromagnetic in advanced applications, 818-821 (2007)
23. J. Holland, *Adaptation in Nature and Artificial System* (Ann Arbor: The University of Michigan Press, 1975).
CST Microwave Studio 2006.b http://www.CST.com.
24. X. Chen, Tomasz, M. Grzegorczyk, B. Wu, J. Pacheco, Jr., and J. A. Kong, "Robust method to retrieve the constitutive effective parameters of metamaterials," Phys. Rev. E **70**, 016608-1-7 (2004).
25. http://www.python.org.
26. F. Bilotti, L. Nucci, and L. Vegni, "An SRR based microwave absorber," Microwave Opt. Technol. Lett. **48**, 2171-2175 (2006).
27. S. Enoch, G. Tayeb, F. Sabouroux, N. Guerin, and P. Vincent, "A Metamaterial for Directive Emission," Phys. Rev. Lett. **89**, 213902-1-4 (2002).
28. D. Schurig, J. J. Mock, and D. R. Smith, "Electric-field-coupled resonators for negative permittivity metamaterials," Appl. Phys. Lett. **88**, 041109-1-3 (2006).

1. Introduction

Recently, there has been growing interest in the study of artificial electromagnetic materials, *metamaterials* [1-15]. Metamaterials are artificially synthesized periodic structures with lattice constant that is much smaller than the wavelength of the incident electromagnetic wave (EM wave), thus considered as effectively homogeneous media [3]. In general, these metamaterials are deliberately designed to manipulate the effective permittivity (ε_{eff}) and permeability (μ_{eff}) of the effectively homogenous media

Of particular interest is the magnetic metamaterial (metaferrites). The first magnetic metamaterial is the split-ring resonator (SRR) proposed by Pendry [2]. The SRR is expected to exhibit resonant magnetic response to the external EM wave, polarizing with the magnetic field parallel to the axis of the SRR (P-polarization). Therefore, the permeability can be negative over a finite frequency range around the resonance frequency. The effective permeability of the periodic arrays of SRR can be characterized by,

$$\mu_{eff}(\omega) = 1 - \frac{\omega_{mp}^2 - \omega_{m0}^2}{\omega^2 - \omega_{m0}^2 + i\Gamma_m \omega} = \mu_{eff}^{'}(\omega) + \mu_{eff}^{''}(\omega), \quad (1)$$

where ω_{0m} is the magnetic resonance frequency, ω_{pm} is the magnetic plasma frequency, and Γ_m is the damping factor.

Furthermore, if both ε_{eff} and μ_{eff} are simultaneously negative, a negative-index metamaterial (NIM), also called left-handed metamaterial (LHM), can be realized [4]. The negative ε_{eff} can be produced by an array of thin metallic wires [1], which behave as the electric resonators. For the electric field of the external EM wave polarizing parallel to the wire, ε_{eff} can be characterized by:

$$\varepsilon_{eff}(\omega) = 1 - \frac{\omega_p^2}{\omega^2}, \quad (2)$$

#91496 - $15.00 USD Received 8 Jan 2008; revised 15 Mar 2008; accepted 17 Mar 2008; published 8 Aug 2008

where ω_p is the electric plasma frequency; the ε_{eff} is predicted to be negative when $\omega < \omega_p$.

A composite material composed of the SRRs and wires can therefore possess negative effective refractive index ($n = \sqrt{\mu_{eff}\varepsilon_{eff}}$) over a finite frequency range, thereby resulting in a NIM.

As a key component of the NIM, the magnetic metamaterials have been extensively studied. Besides the SRR, a number of candidate magnetic resonant structures have been proposed; these include hexagonal split-ring resonators [10], S-shaped resonators [11], double S-shaped resonators [12], Ω-shaped resonators [13], quasi-periodic dendritic-cell [14], and labyrinth resonators [15]. The traditional magnetic metamaterial design is based on the analysis of the equivalent LC-circuit, consisting of the plate capacitors and magnetic coils on a scale much smaller than the wavelength of incident wave [2]. However, this may be very complicated for irregular shapes and therefore restrict the magnetic metamaterial to regular shape. It is also difficult to find the optimal structures for the magnetic or other functional metamaterials using the intuition and empirical testing. To solve this problem, we, in this paper, intend to propose an intelligent computer-aided design (CAD) approach employing the genetic algorithm (GA) and the filling element methodology to synthesize the magnetic metamaterials with whatever regular or irregular structures. A representative design example, magnetic metamaterial with a desired permeability value of μ_{eff} = -1, is detailed. For the filling element structural design methodology, we use the typical filling square-pixel (FSP) method and a novel filling beehive-cell (FBC) method, which aims at improving the patch contact problem in the FSP method. Furthermore, different types of the magnetic and electric metamaterials with different desired material properties are studied to illustrate the versatility and applicability of our approach for the metamaterial synthesis designs. A more detailed implantation of the GA-optimization for the structural design of metamaterials will be described in the following section.

2. Genetic algorithm and structural design

The principle of how to automatically generate structures by computer is illustrated in Fig. 1; Fig. 1(a) shows the typical FSP method, which has widely been used for structural design problems [16-17]; Fig. 1(b) shows the novel FBC method. For comparison, both methods will be used to synthesize a unit cell of the metamaterial. The incident field propagates along the *x*-direction, with **E** and **H** along the *x*- and *y*-directions, respectively. The metamaterial is formed by the elementary metallic patches printed on one side (*x*-*z* plane) of the dielectric substrate, which is a 1.5-mm-thick FR4 with relative permittivity ε_r = 4.4. Since our interest frequency is in the range of 4~10 GHz, the artificial lattice constant is $a_x = a_y = a_z$ = 7.5 mm, which assures to be 1/4 ~ 1/10 the wavelength of the EM wave. We then discretize the unit cell into many elements (square-pixels or beehive-cells); each element can be filled by metal or in free space (ε_0 = 1). Here we define N_s and N_c as the number of elementary patches at each side for the FSP and FBC method, respectively. The structure is forced to be mirrored to ensure the 1D-symmetry of the metamaterial (see Fig. 1). Although this CAD approach seems to be ideal and a wide variety of structures can be discovered, the most critical problem is that the total number of possible structures is extremely huge. Take the FSP method for example, the total number of possible structures is $2^{Ns(Ns+1)/2}$ (i.e. for N_s = 7, there are more than 2.6×10^8 different structures) and it will increase exponentially with the number of pixels. Therefore, the full search method is not practical, especially when the number of the elements is very large. In this work, the simulation experiments of $N_s = N_c$ = 7 and 11 are performed. The search space would be 49-pixel and 21-pixel square patch for N_s = 7 and 11, respectively, and that would be 37-cell and 91-cell beehive for N_c = 7 and 11, respectively. For problems involving such a large search space, it is also impossible to land the result in the global optimum by the gradient-based local search method. As a result, the GA, as a direct and adaptive search technique, should be introduced to automatically generate the optimal

#91496 - $15.00 USD Received 8 Jan 2008; revised 15 Mar 2008; accepted 17 Mar 2008; published 8 Aug 2008

structure. The GA is a very powerful and attractive optimization tool, and has been applied to several electromagnetic problems, such as the microwave antennas [16], photonic crystals [18-19], ion-optics [20], and some metamaterial designs even in the synthesis design of metamaterials by FSP method [17] or automatic parameter extraction [21-22].

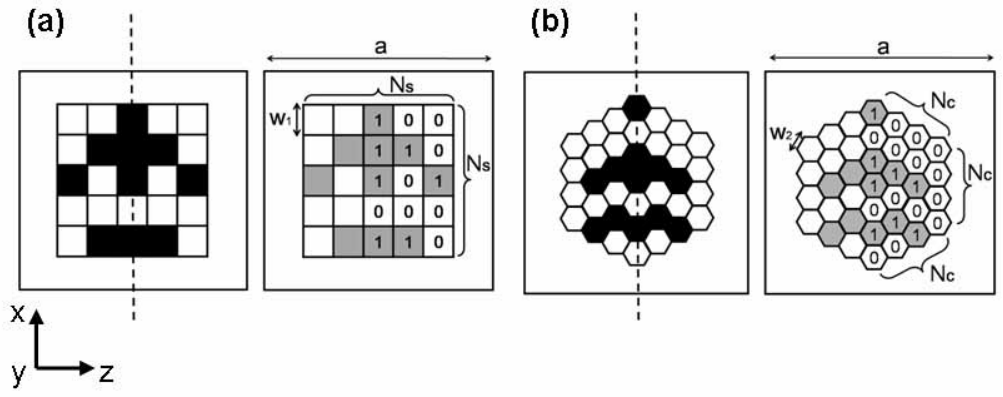

Fig. 1. Illustration of (a) filling square-pixel (FSP) and (b) filling beehive-cell (FBC) method for the structural design of a metamaterial unit cell. The lattice constant $a_x = a_y = a_z = a$ is set to 7.5mm. The dimensions of the metallic patches are $w_1 = 0.8$ mm, $w_2 = 0.55$ mm for $N_s = N_c = 7$, and $w_1 = 0.5$ mm, $w_2 = 0.35$ mm for $N_s = N_c = 11$.The thickness of the substrate (FR4 with $\varepsilon_r = 4.4$) and the metallic patches are 1.5 mm and 0.035 mm, respectively.

The idea of the GA came from Charles Darwin's theory of evolution, natural selection or survival of the fittest [23]. In the GA, the structure of the metamaterial is encoded using a binary string filled with "1's" and "0's" representing metal and free space, respectively (see Fig. 1). This binary string is called "chromosome" and each 1's and 0's on the chromosome can be seen as a "gene." At the start of GA, $N_{chromosome}$ (here $N_{chromosome} = 80$) chromosomes are randomly generated (each gene on the chromosome is randomly set to 1's and 0's with the uniform probability) to form the initial population, $\mathbf{G_0}$. Each chromosome is then assigned a fitness value, F, providing an indication of quality of chromosome to determine whether this chromosome is the most probable to evolve towards a better next generation. Under the pressure of the fitness, GA will evolve, over time, toward the optimal solution. The fitness is defined as:

$$fitness = \min\left(|\mu_{eff}^{'} + R_a| + |\mu_{eff}^{''} + R_b|\right)\Big|_{4\,GHz < f < 10\,GHz} \tag{3}$$

where $\mu_{eff}^{'}$ and $\mu_{eff}^{''}$ represents the real part and the imaginary part of μ_{eff}. Since our goal aims at producing negative magnetic metamaterial with $\mu_{eff} = -1$, we must choose $R_a = 1$ and $R_b = 0$. We note that the imaginary part determines the absorption of the EM wave. Hence, for low loss, the real part should be negative unity while at the same time the image part should be zero. The commercial available software, CST Microwave Studio [24], is employed as the Maxwell's equation solver, which is a finite-different time-domain (FDTD) simulation based on perfect boundary approximation and finite integration technique. The metallic patches with the thickness of 0.035 mm are modeled as PEC because in our interest frequency range the effect of the skin depth (δ~0.7 μm) can be neglected. Due to the periodicity of the metamaterials, we limit our simulation to a single unit cell with periodic boundary condition. After the transmission and reflection coefficients of each chromosome are calculated, the robust retrieval method [25] is applied to compute the effective impedance z, the effective refractive index n, and effective permittivity ε_{eff}, and the effective permeability μ_{eff} of the metamaterial.

#91496 - $15.00 USD Received 8 Jan 2008; revised 15 Mar 2008; accepted 17 Mar 2008; published 8 Aug 2008

Based on the fitness value given in Eq. (3), the next generation is produced by the "reproduction" process utilizing the biologically analogous operators of *selection* (**S**), *crossover* (**C**), and *mutation* (**M**). In these steps, we define $\mathbf{G^k}$ and $\mathbf{G^{k+1}}$ as the current and the next generations, respectively. The operation steps of GA are described as follows:

(i) *Selection*: in this step, a pair of chromosomes is selected from the current generation as parents for mating. Here the tournament selection strategy is used, four chromosomes are randomly chosen and the best two individuals are selected as the parents. Therefore, chromosomes with higher fitness values are more likely to be selected for generating new chromosomes or children.

(ii) *Crossover*: once the parents are selected, two chromosomes will interchange their gene material, with a crossover probability P_c = 0.8, to create a pair of children. Here, we use the two-point crossover strategy, in which the parents will exchange the segments cut by two randomly selected points to create two children. The purpose of crossover is to rearrange the genes, thereby creating better combinations of genes to result in "fitter" chromosome.

(iii) *Mutation*: mutation is also necessary to maintain the diversity in the population and explore the solutions which are not yet present, thus preventing the results to be trapped in the local minimum. Here, we use the uniform mutation, in which each gene could be mutated under a mutation probability P_m= 0.08. In the case of binary coding "1s" will be inverted to "0" and vice versa.

(iv) *Elitist strategy*: the top 5% chromosomes, as the "elite chromosomes," from the current generation are preserved and directly inserted into a new generation. This procedure ensures the elite of each population survive to be used as the parents in the next generation.

These processes, including selection, crossover, and mutation are repeated until the size of the new generation is the same as the current generation. The relationship of the next generation and the current generation can be described as $\mathbf{G_{k+1}} = \mathbf{M}\{\mathbf{C}\{\mathbf{S}\{\mathbf{G_k}\}\}\}$. The GA processes are iterated until N_g (here N_g = 50) generations are calculated. Since the GA's result cannot guarantee the global optimum, three runs with different randomly generated initial population are performed and the best chromosome is saved. A computer intelligence technique framework, *CITO lab*, included the GA and middleware between the GA and the CST Microwave Studio, has been developed at National Nano Device Laboratories (NDL). This framework is completely written in the open-source programming language, Python [26].

3. Results and Discussion

Figure 2 shows the best fitness as a function of the number of generations. For all cases, it is seen that the best fitness eventually converges to a fixed value. The corresponding optimized structures for the FBC design at different generations during the evolution process of the GA are shown in the bottom of Fig. 2. For FBC method with N_c = 7, the structure is eventually evaluated to a structure that is analogous to the typical double SRR, having one outer ring and one inner ring with oppositely-oriented splits. The insert of inner ring is to generate a large capacitance in the small gap between two rings, thus lowering the resonance frequency and concentrate the electric field to enhance the response [3]. It is surprising that the GA has such an ability to find out an optimized structure, nearly consisting with that designed by people. This also implies that double SRR might be the best suitable for FBC method with small number of elements (spatial resolution). It is also found from Fig. 2 that the value of the best fitness decreases with increasing the number of elements (search space is enlarged). This is valid for both the FSP and FBC methods.

#91496 - $15.00 USD Received 8 Jan 2008; revised 15 Mar 2008; accepted 17 Mar 2008; published 8 Aug 2008

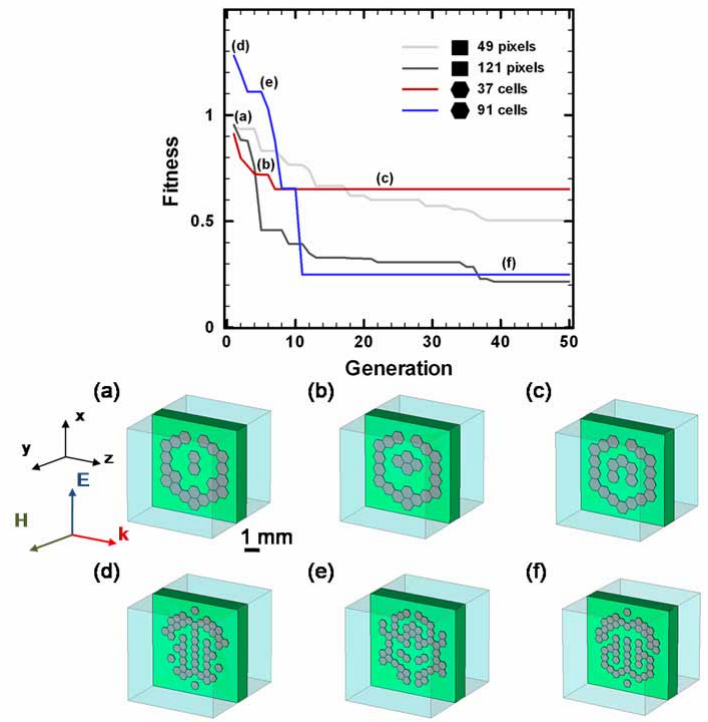

Fig. 2. The best fitness plotted as a function of generation (top). The unit cells show the best structures (elite) at different generations during the evolution process of the GA (bottom).

Applying the GA with different structural design methodology, different GA-optimized structures are shown in Fig. 3. Figures 3(a) and (b) show the resulting structures using the FSP method with $N_s = 7$ and $N_s = 11$, respectively. The corresponding μ_{eff} and ε_{eff} are also shown in the right-hand side. In both cases, a symmetrical ring structure with a large capacitance at the split is presented. It is not hard to image that a symmetric ring with a distinct capacitance and an inductance will form a LC-circuit to response to the external magnetic field of the EM wave, thus producing the magnetic resonance. A typical resonant behavior in $\mu_{eff}(\omega)$ can be clearly seen in both Fig. 3(a) and (b). At resonance, a considerably large positive μ_{eff} in the low frequency side of the resonance and negative μ_{eff} in the high frequency side of the resonance are obtained. In addition, an antiresonant behavior [7] of ε_{eff} accompanied with the resonant behavior of μ_{eff} is shown, in which the imaginary parts of μ_{eff} and ε_{eff} are opposite in sign. For $N_s = 7$ the optimal values of μ_{eff} is given by $\mu_{eff} = -0.965 + i0.469$ (*fitness* = 0.504) at 4.25 GHz, while for $N_s = 11$ an improved optimized value of μ_{eff} is given by $\mu_{eff} = -0.992 + i0.208$ (*fitness* = 0.216) at 4.05 GHz.

#91496 - $15.00 USD Received 8 Jan 2008; revised 15 Mar 2008; accepted 17 Mar 2008; published 8 Aug 2008

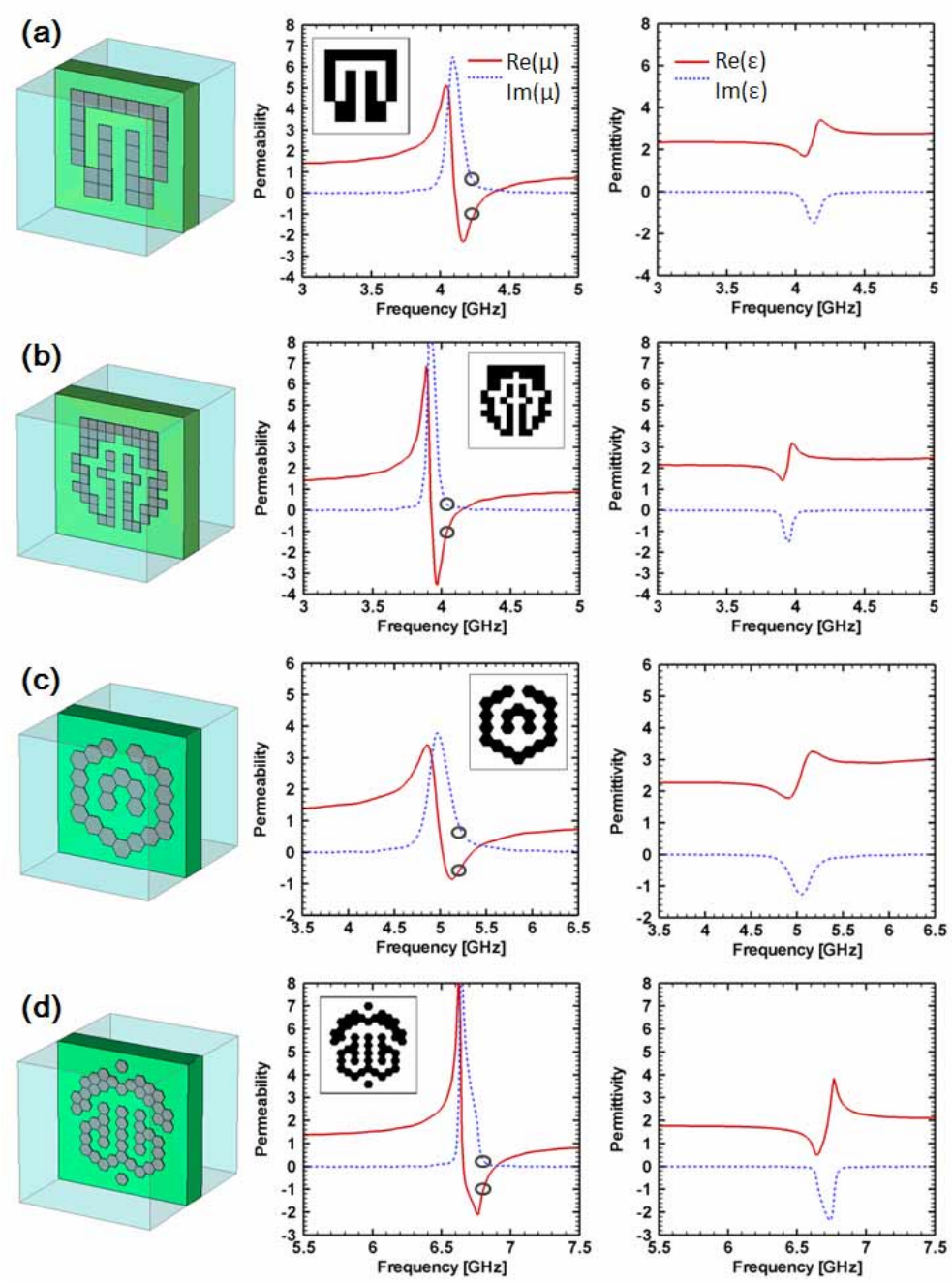

Fig. 3. GA-optimized unit cell and its corresponding μ_{eff} and ε_{eff} for the FSP method with (a) N_s = 7 and (b) N_s = 11, and the FBC method with (c) N_c = 7and (d)N_c = 11 (desired permeability: μ_{eff} = -1 over the range of 4~10 GHz).

Figures 3(c) and (d) show the resulting structures and the corresponding μ_{eff} and ε_{eff} using the FBH method with N_c = 7 and N_c = 11, respectively. For N_c = 7, the double SRR-like structure is presented. The optimized values of μ_{eff} is given by μ_{eff} = -0.668 + *i*0.319 (*fitness* = 0.651) at 5.2 GHz. However, for N_c = 11, a more complex resonant structure, as shown in Fig. 3(d), is presented, in which several capacitors and inductors are shunted together to form a

#91496 - $15.00 USD Received 8 Jan 2008; revised 15 Mar 2008; accepted 17 Mar 2008; published 8 Aug 2008

LC-circuit, thus producing the magnetic resonance. As compared to the case of N_c = 7, this complex structure has a stronger resonant behavior as well as an enhanced magnitude of μ_{eff}. The optimized value of μ_{eff} for N_c = 11 has been improved to μ_{eff} = -1.011 + *i*0.237 (*fitness* = 0.248) at 6.8 GHz. The resonance frequency increases because more capacitive elements are shunted to build up the magnetic resonator. This phenomenon is analogous to that in multi-cut SRR: the resonance frequency increases with increasing the number of cuts of SRR.

Comparing two structural design methods, there are advantages for the FBC method. Firstly, the electric connection problem for two diagonally-neighbor elements in the FSP method can be improved. Moreover, for both small and large number of elements, the FBC design is found to result in a faster convergence speed than that of the FSP design. This is because the computer-generated pattern by the FBC method is much easier to evaluate toward a closed and conductive circuit due to the nature of beehive. As a result, the FBC method can improve electric connection, while at the same time, yield to a faster convergence speed. The single-processor execution time for the fitness evaluation (CST simulation) of a chromosome takes approximately 1.5~2 minutes (depends on the complexity of the structures) on a HP Pentium IV-3.06 GHz PC with 3.37GB RAM.

Based on the same concept in the prior example, we further use the GA to synthesize the magnetic metamaterials with the desired permeability values of μ_{eff} = -0.5 and μ_{eff} = -2 over the same frequency range. Here the value of R_a in fitness function (Eq. 3) is replaced by R_a = 0.5 and R_a = 2 to achieve the design goals of μ_{eff} = -0.5 and μ_{ef} = -2, respectively. In the following, the FBC method will be used throughout this study.

Figure 4 shows the resulting structure and the corresponding μ_{eff} and ε_{eff} of the magnetic metamaterial with a desired permeability μ_{eff} = -0.5. The optimized values of μ_{eff} is given by μ_{eff} = -0.470 + *i*0.055 (*fitness* = 0.085) at 7.02 GHz.

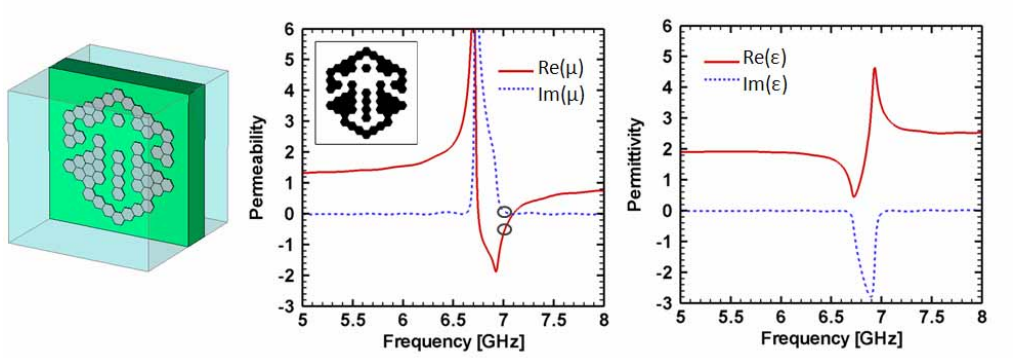

Fig. 4. The GA-optimized unit cell for the metamaterial with permeability μ_{eff} = -0.5 and its corresponding μ_{eff} and ε_{eff}.

Figure 5 shows the resulting structure and the corresponding μ_{eff} and ε_{eff} of the magnetic metamaterial with a desired permeability μ_{eff} = -2; the optimized values of μ_{eff} is given by μ_{eff} = -1.955 + *i*0.448 (*fitness* = 0.493) at 5.53 GHz. To obtain a larger negative value of permeability, the magnitude enhancement of μ_{eff} is required. As can be seen in Fig. 5, the magnetic resonance becomes stronger as compared to the prior case.

#91496 - $15.00 USD Received 8 Jan 2008; revised 15 Mar 2008; accepted 17 Mar 2008; published 8 Aug 2008

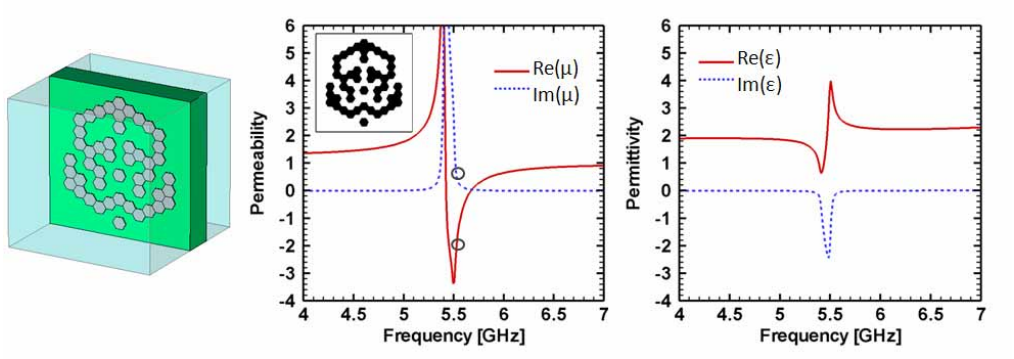

Fig. 5. The GA-optimized unit cell for the metamaterial with permeability μ_{eff} = -2 and its corresponding μ_{eff} and ε_{eff}.

In contrast to the negative and low-loss magnetic metamaterials, a metamaterial with positive and large μ'_{eff} and μ''_{eff} can also be obtained in the low frequency side of the magnetic resonance. Therefore, magnetic metamaterial can also act as an effective electromagnetic absorber at the desired operating frequency [27]. This encourage us to use the GA to synthesize a lossy magnetic metamaterial with permeability μ_{eff} = 2+ *i*4. In this case, R_a = -2 and R_a = -4 is applied. Fig. 6 shows the resulting structure and the corresponding μ_{eff} and ε_{eff} of such a metamateria is given by μ_{eff} = 2.067 + *i*4.025 (*fitness* = 0.092) at 5.08 GHz.

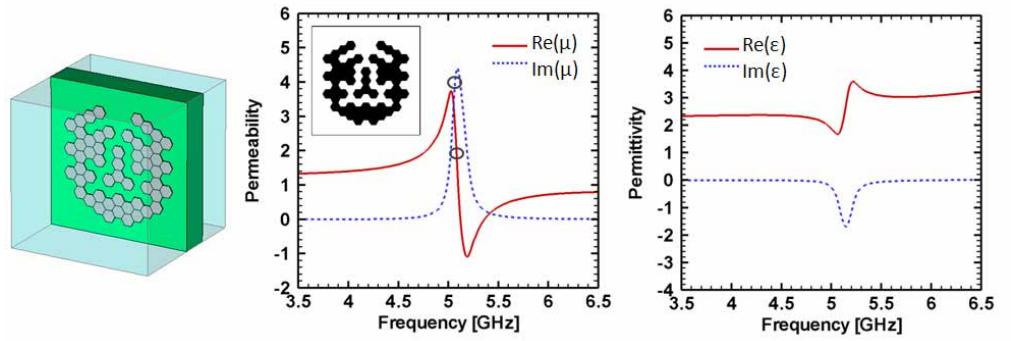

Fig. 6. The GA-optimized unit cell for the metamaterial with permeability μ_{eff} =2 + *i*4 and its corresponding μ_{eff} and ε_{eff}.

So far, the object in all cases aims to search the optimized structure in terms of the desired permeability for all frequencies between 4 GHz and 10 GHz. Next, we intend to use the GA to synthesize a particular magnetic metamaterial at a fixed frequency under the same unit cell size. Here we take the design of a magnetic metamaterial with μ_{eff} = -1 at 5 GHz for example. In this case, the fitness is defined as:

$$fitness = \min\left(|\mu'_{eff} + 1| + |\mu''_{eff}|\right)\Big|_{f=5GHz} \quad (5)$$

Figure 7 shows the resulting structure and the corresponding μ_{eff} and ε_{eff}. From Fig. 7, we can find that, at 5.0 GHz, μ_{eff} = -0.970 + *i*0.506 (*fitness* = 0.536) is obtained.

#91496 - $15.00 USD Received 8 Jan 2008; revised 15 Mar 2008; accepted 17 Mar 2008; published 8 Aug 2008

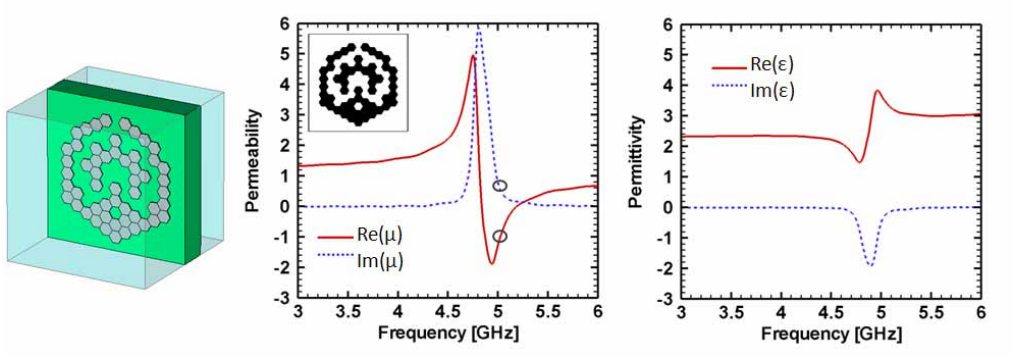

Fig. 7. The GA-optimized unit cell for the metamaterial with permeability μ_{eff} = -1 at 5 GHz and its corresponding μ_{eff} and ε_{eff}.

In addition to the NIMs, there is also increasing interest in the zero-index and low-index metamaterials (ZIMs, LIMs) due to their fascinating physical properties and potential applications, such as the high directivity antenna according to Snell's refraction law [28] and metamaterial invisibility cloak [9, 21]. In these applications, like the operation of NIMs, zero or low refractive index are tuned through the manipulation of the μ_{eff} and ε_{eff}. Here we take μ_{eff} = 0 as a design example to testify GA's capability of synthesis functional metamaterial, but alter the fitness function to:

$$fitness = \left(|\mu_{eff}^{'}| + |\mu_{eff}^{''}| \right) \Big|_{\mu_{eff}^{'} = \min(\mu_{eff}^{'})} \tag{6}$$

Our purpose is to design a zero or low permeability metamaterial. The resulting metamaterial and its μ_{eff} and ε_{eff} are shown in Fig. 8, where the minimum μ_{eff} saturates to zero at the high frequency side of the resonance and its value is 0.086 + i0.595 (*fitness* = 0.681) at 6.52 GHz.

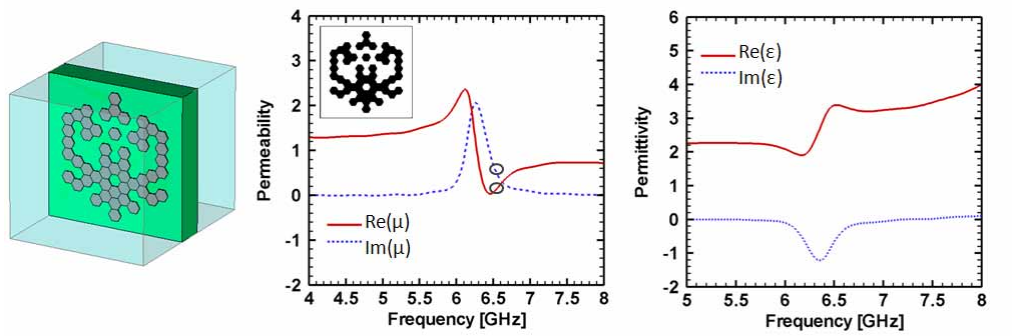

Fig. 8. The GA-optimized unit cell for the metamaterial with permeability of zero and its corresponding μ_{eff} and ε_{eff}.

Since metamaterials are usually composed of strong magnetic or electric resonant structure, in the last part, we would like use the GA to synthesize an electric-LC (ELC) resonator with ε_{eff} = -1and a NIM or LHM with n = -1. We note that the electric metamaterial, as a discontinuous metallic pattern, could also possess a cut-wires-like electric resonant behavior [8]. The effective permittivity can characterized as:

$$\varepsilon_{eff}(\omega) = 1 - \frac{\omega_{ep}^2 - \omega_{e0}^2}{\omega^2 - \omega_{e0}^2 + i\Gamma_e \omega} = \varepsilon_{eff}^{'}(\omega) + \varepsilon_{eff}^{''}(\omega) \tag{4}$$

#91496 - $15.00 USD Received 8 Jan 2008; revised 15 Mar 2008; accepted 17 Mar 2008; published 8 Aug 2008

where ω_{e0} is the electric resonance frequency, ω_{ep} is the electric plasma frequency, and Γ_e is the damping factor. When an electric metamaterial with a desired permittivity ε_{eff} = -1 is considered, we should define the fitness as:

$$fitness = \min\left(|\varepsilon'_{eff} + 1| + |\varepsilon''_{eff}|\right)\Big|_{4\,GHz < f < 10\,GHz} \quad (7)$$

The resulting metamaterial structure and its ε_{eff} and μ_{eff} are shown in Fig. 9. During the electric resonance, the optimized values of ε_{eff} is found to be -1.011 + i0.001 (*fitness* = 0.012) at 7.63 GHz. From Fig. 9, a resonant behavior similar to the magnetic resonance but in $\varepsilon_{eff}(\omega)$ is clearly seen. The antiresonant behavior of μ_{eff} accompanied by the resonant behavior of ε_{eff} is also observed.

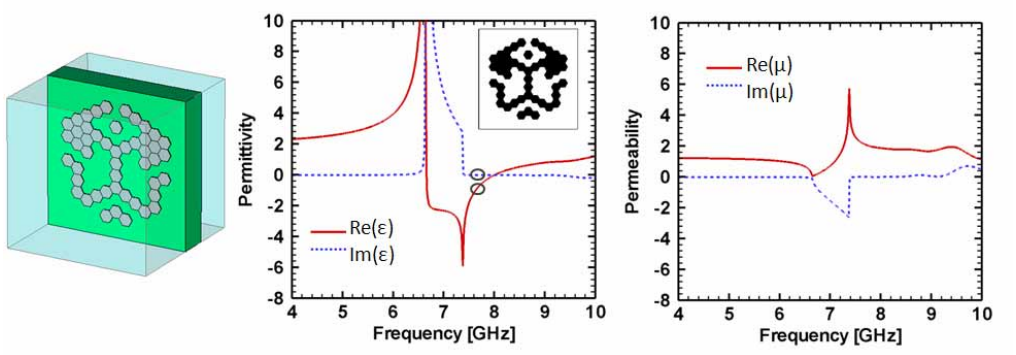

Fig. 9. The GA-optimized unit cell for the metamaterial with permittivity of ε_{eff} = -1 and its corresponding ε_{eff} and μ_{eff}.

We further construct a composite material consists both the magnetic and electric resonator on the opposite sites of the dielectric substrate for making a NIM. With the magnetic resonator from Fig. 3(d) on the back site of the substrate, we use the GA to synthesize an electric resonator on the top site. Hence, the refractive index is expected to be negative through the combination of the electric resonator with $\varepsilon_{eff} < 0$ and the magnetic resonator with $\mu_{eff} < 0$. To this end, the fitness is defined as:

$$fitness = \min\left(|n'_{eff} + 1| + |n''_{eff}|\right)\Big|_{4\,GHz < f < 10\ \ GHz} \quad (8)$$

Figure 10 shows the optimized NIM as well as the retrieval μ_{eff}, ε_{eff}, *n* and *z*. At 6.90 GHz, n = -1.109 + *i*0.326 (fitness = 0.435) is obtained. We note that a dual-band is found in the curve of μ_{eff}. The first magnetic response, which is caused by the electric resonator on the top site, is weak (the peak is slightly below zero). This has been verified by removing the magnetic resonator on the back site. The second response at the negative-index frequency region is actually produced by the magnetic resonator.

#91496 - $15.00 USD Received 8 Jan 2008; revised 15 Mar 2008; accepted 17 Mar 2008; published 8 Aug 2008

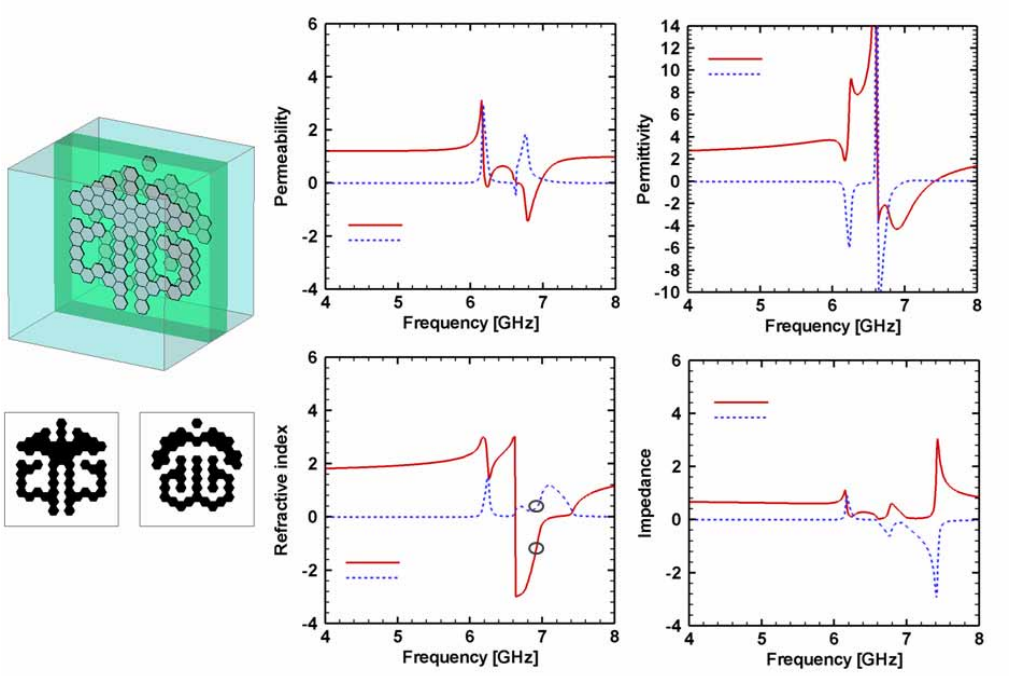

Fig. 10. Left-handed side shows the unit cell of a NIM, which is composite material made of the GA-optimized electric and magnetic resonators on the opposite sides of the substrate; the right-handed side shows its corresponding μ_{eff}, ε_{eff}, n and z.

So far we have demonstrated the possibility, stability as well as flexibility of using AI, such as the GA in this paper, to design metamaterial with the permeability or permittivity almost fit to the desired values. We note that the difference between the fitness (simulated result) and the design goal (desired material properties) can be further reduced by optimizing the fixed design parameters for each GA-optimized structure, such as the size of the unit cell a and metallic patch w, the thickness t and permittivity of the dielectric substrate ε_r. The GA-optimized structures can promise to be fabricated by the standard circuit board lithography. Although, in this work, GA is employed to make metamaterial in the microwave region, these results have also implications for other regions of the electromagnetic spectrum, such as infrared or even optical frequencies. Our design approach would also potentially enable us to design versatile functional metamaterials not presented here (i.e. low-loss, high-absorption, dual-band, or wide-band ($\Delta f / f$) metamaterial at the desired frequencies).

4. Conclusion

We have illustrated that the GA can work well in the synthesis of the metamaterials with permeability of negative unity. Two structural design methodologies, the typical FSP and the novel FBC methods, are performed and the stability of the GA has been proved in both cases. It is also worth mentioned that the FBC method can improve electric contact problem and give a faster convergence speed, while the performance of the resulting structure is comparable to that by using the FSP method. To further demonstrate the stability and flexibility of our design approach, using the GA and FBC method, various metamaterials are synthesized; these include four low-loss magnetic metamaterials with permeability μ_{eff} = -0.5, -2 and 0, a lossy magnetic metamaterials with permeability μ_{eff} = 2 + 4i, an electric metamaterial with permittivity ε_{eff} = -1, and a NIM with refractive index n = 1. All these cases can be synthesized successfully with the material properties approximate to our design goals. With this intelligent CAD technique, we are able to design the functional metamaterials with the desired material

#91496 - $15.00 USD Received 8 Jan 2008; revised 15 Mar 2008; accepted 17 Mar 2008; published 8 Aug 2008

properties according to the user-defined object function (fitness function in the GA). Such encouraging results have shed bright light on using artificial intelligence to make artificial metamaterials.

Acknowledgments

The authors acknowledge Prof. C. T. Sun of Department of Computer Science, National Chiao Tung University, Taiwan for discussions in genetic algorithm, evolutionary computation, and system development. We also want to thank Prof. T. J. Yen of Department of Material Science Engineering, National Tsin Hua University, Taiwan for the help in CST simulation. This work is funded by National Nano Device Laboratory, Taiwan.

#91496 - $15.00 USD Received 8 Jan 2008; revised 15 Mar 2008; accepted 17 Mar 2008; published 8 Aug 2008